Geometric Stability and Elastic Response of a Supported Nanoparticle Film

Brian D. Leahy,[1] Luka Pocivavsek,[2,3] Mati Meron,[1] Kin Lok Lam,[2] Desiree Salas,[2] P. James Viccaro,[1,2] Ka Yee C. Lee,[2,3] and Binhua Lin[1,2,*]

[1]*Center for Advanced Radiation Sources, University of Chicago, Chicago, Illinois 60637, USA*
[2]*James Franck Institute, University of Chicago, Chicago, Illinois 60637, USA*
[3]*Department of Chemistry and Institute for Biophysical Dynamics, University of Chicago, Chicago, Illinois 60637, USA*
(Received 22 October 2009; published 30 July 2010)

The mechanical response to compression of a self-assembled gold nanoparticle monolayer and trilayer at the air-liquid interface is examined. Analysis of the film's buckling morphology under compression reveals an anomalously low bending rigidity for both the monolayer and the trilayer, in contrast with continuum elastic plates. We attribute this to the spherical geometry of the nanoparticles and poor coupling between layers, respectively. The elastic energy of the trilayers is first delocalized in wrinkles and then localized into folds, as predicted by linear and nonlinear elastic theory for an inextensible thin film supported on a fluid.

DOI: 10.1103/PhysRevLett.105.058301 PACS numbers: 68.55.J−, 68.60.Bs

Films of nanoparticles at an interface exhibit rich behavior, determined by the material properties of the nanoparticles as well as the thermodynamic and mechanical responses of interfacial structures [1]. Mechanical properties of the nanoparticle superlattice are tunable, for example, by altering the ratio of the core to the ligand length [2] or by changing the composition of the solution [3]. In addition, nanoparticles scatter radiation very strongly. These make them ideal model systems for studying the properties of compressed nanometer-thin films at interfaces, allowing a large variety of predictions for response to stress [4,5] and the effects of confinement or defects [6] to be tested *in situ*. In this Letter, we report on the mechanical response to compression of a self-assembled gold nanoparticle film at the air-liquid interface.

Over the past two decades, energy balance and scaling arguments [5,7,8] have proven fruitful in describing and predicting the elastic behavior of thin plates under lateral compression. The canonical approach is to divide the elastic energy of the plate into components containing in-plane strains ϵ (called ''stretching'') and those generated by development of curvatures κ (called ''bending'') [7]. Often, for plates whose thickness is much smaller than their lateral dimensions, only bending energies (U_B) need to be considered when evaluating the elastic stability of the system [7]. For a plate bound to a fluid substrate, the deformation (z) of the substrate also costs energy (U_K). The total energy in the linear approximation is

$$U = U_B + U_K = \frac{1}{2}\int (B\kappa^2 + Kz^2)dA, \qquad (1)$$

where B is the bending rigidity of the plate and K is the stiffness of the substrate. Equation (1) is minimized by balancing the bending energy and the deformation energy, while approximating the plate as inextensible [5,8–10]. Such a balance selects the equilibrium shape of the interface, with the surface forming stable wrinkles with a wavelength of

$$\lambda = 2\pi(B/\rho g)^{1/4} \qquad (2)$$

[4,8,10]. Here K is replaced by ρg, where ρ is the density and g the gravitational acceleration [5,10]. For large deflections, the energy of the system localizes into folds. This has been described using a nonlinear geometric term added to Eq. (1), suggesting that the subducted length l of the fold scales as the wrinkle wavelength λ: $l \sim \lambda$ [5,9].

The simple elastic model described above needs to be further tested before it is applied to nanometer-thin films on fluid subphases, especially for films of discrete particles. Surface tension or viscosity, ignored in Eq. (1), might play a role in the film's response to compression. For example, Huang and Suo [11] have shown that viscous effects alone can cause wrinkling in supported thin films. For thin films at an interface, surface energies can become much larger than mechanical energies (e.g., U_B and U_K) and may play a role in the films' response. We observe that our system can be described by the energetic scaling approach in Eqs. (1) and (2). We measure the film's bending rigidity and find it anomalously low compared to a continuous plate, which can be attributed to the unique structural properties of the spherical particle film.

A Langmuir trough (NIMA) with two barriers was used to prepare the gold nanoparticle film. To make the film, 6 nm gold nanoparticles ligated with dodecanethiol (Ocean Nanotech) and suspended in heptane were spread at the air-liquid interface. The morphology of the film was then imaged continuously with an Olympus light microscope and recorded for the duration of the compression [12].

Driven by ligand interactions [2], the nanoparticles aggregate into islands of solid monolayer [3] tens of microns to many millimeters across, surrounded by a bare air-liquid interface [Fig. 1(a)] [12]. The monolayer is then compressed laterally, using two barriers. The nanoparticle islands rearrange under compression in the x direction to form a continuous monolayer.

Upon further compression, the monolayer enters the third dimension (z). Figure 1(b) shows the appearance of a crisscross "hash" pattern on the surface, composed of jagged lines darker than the surrounding monolayer. Using atomic force microscopy (AFM), we measured the height profiles of films with hash [Fig. 2(a)] by transferring the nanoparticle film from the air-water interface to a graphite puck [13,14]. The height profiles show the hashed lines raised 11.1 ± 1.8 nm, or two particle diameters, above the surrounding 6 nm thick monolayer. This indicates that the monolayer collapses into trilayers 17 nm thick. Our *in situ* x-ray measurements at similar compressive strains [3] have also revealed that the gold nanoparticle monolayer and trilayer coexist. Because the collapse structure (i.e., hash) is 3 nanoparticle layers thick (within the precision of x-ray and AFM measurements), and no other thicknesses were measured, the most plausible mechanism is that the monolayer folds sideways (S folds), giving rise to stripes of trilayers as illustrated in Fig. 2. As compression continues, the hash lines become denser and align nearly perpendicular to the direction of compression. Ultimately, the surface film completes its transition from a monolayer to an optically homogeneous trilayer [Fig. 1(d)].

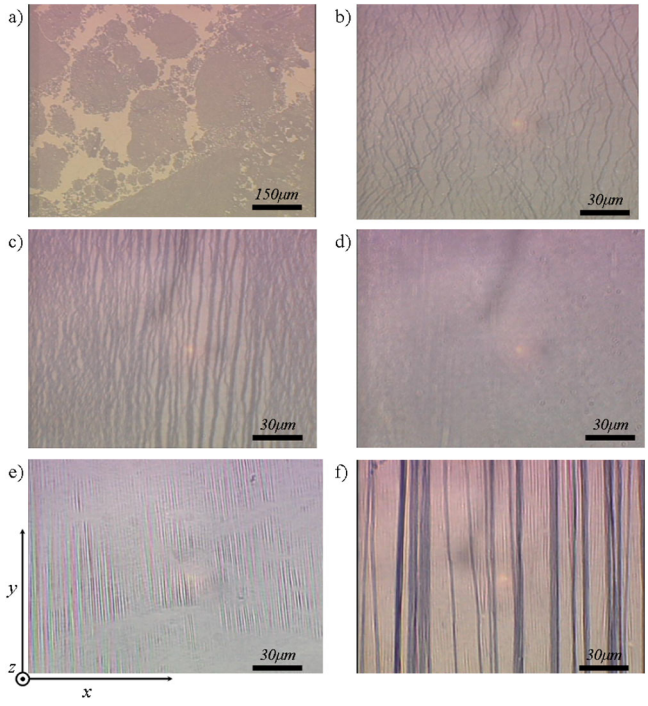

FIG. 1 (color online). (a) The gold nanoparticles initially form islands of monolayer on the water interface. The nanoparticle film is purple in the image; the surrounding air-water interface appears bright. Compressing in the x direction rearranges these islands into an optically continuous monolayer. Further compression forces the monolayer to S fold into a trilayer, appearing as a dark hash on the surface (b). As compression continues, more of the film undergoes the hash transition (c), eventually bringing the film to a continuous trilayer (d). Compacting the trilayer causes it to wrinkle (e). Continued confinement increases wrinkle amplitudes until vertical folding starts to occur. (f) The trilayer when many wrinkle-to-fold transitions have occurred. Notice that the film still wrinkles with the same periodicity.

The trilayered film responds to compression by forming static, periodic wrinkles oriented along the y direction [Fig. 1(e)]. Unlike the hash, wrinkles appear in a single direction perpendicular to compression and do not change direction over their length. They occur in groups extending tens to hundreds of microns in the y direction. The periodicity of the wrinkles on the film was measured over 300 wavelengths, showing a uniform wavelength λ of 2.7 ± 0.5 μm. Note that the wavelength is independent of applied strain. The wrinkles are stable when compression is stopped, but quickly dissipate upon decompression.

Continued compression of the wrinkled surface causes it to fold vertically into the subphase, i.e., in the $-z$ direction. These vertical folds (V folds) are localized, having widths of only a few microns. V folds have a well-defined orientation and extend in the y direction from hundreds of microns to a few centimeters [Fig. 1(f)]. We characterize these folds by their subducted length l. The distance between visible marks on the film on either side of a nascent fold was measured immediately before and after the fold nucleated; this difference plus the fold width was interpreted as l. Most V folds have an l of about 5–9 μm, as measured over approximately 30 folds [12]. This is the mode; the distribution is right-skewed. The V folding events are rapid; a typical event, from nucleation to formation, lasts ~100 ms. Additional compression results in more wrinkle-to-fold transitions throughout the film.

The geometry of a supported elastic sheet under compression contains information about its material properties. We deduce the mechanical properties of the nanoparticle monolayer from its buckling into trilayers. To fold into the observed three-particle-thick trilayer, the monolayer must first bend with a curvature of $\kappa \sim 10^9$ m^{-1}. The presence

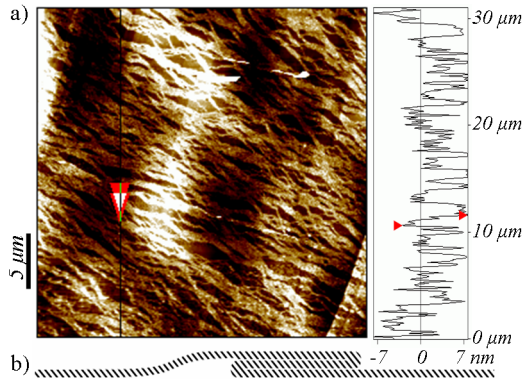

FIG. 2 (color online). (a) AFM height profile of a 30 × 30 μm section of the film late in the monolayer-to-trilayer transition. At right is a height profile of the line in the image. The height difference between the two red arrows is 11.7 nm, corresponding to that between a monolayer and a trilayer. Note the quantization of the height profile; the difference in height is consistently 2 particle diameters (≈12 nm). (b) A schematic of an S fold and how it could cause trilayer formation.

of such high curvatures suggests that the monolayer has a very low bending rigidity. However, this does not preclude a high Young's modulus (E). The bending rigidity of an object is determined by both its Young's modulus and its structure. For a continuous plate of thickness t and Poisson's ratio ν, B is determined by the resistance to stretching and compressing of the individual stratum in the plate. Summing the moments from each layer gives the familiar result $B = Et^3/12(1-\nu^2)$ [15]. If the plate is not continuous, e.g., with a discrete structure like chain mail, then this relation breaks down. In the limiting case of a monolayer, B is determined by the resistance to bending of the individual particles. For an asymmetric molecule like a phospholipid, the continuum relation may still hold [16]. For a monolayer composed of radially symmetric particles such as the gold nanospheres, bending does not cause local stretching or compression as nearby spherical particles can rotate freely with respect to each other. The monolayer can therefore have an anomalously low B while still maintaining a sizable E.

We can estimate the Young's modulus of the gold nanosphere monolayer from the measured surface pressure [12] in the region between the formation of the monolayer and the onset of buckling, by assuming that the monolayer obeys Hooke's law before buckling into a trilayer. For such a scenario, $\sigma/\epsilon = Et$, where σ is the surface pressure and ϵ the strain [15]. Using the maximal pressure attained in this region, 20 mN/m, and the corresponding strain of 10% yields a value for E of about 40 MPa. The estimated E for our system does not necessarily contradict higher values of $E \approx 0.1-1$ GPa previously reported from simulations or an experiment on a freestanding gold nanoparticle monolayer [2,17], nor does it suggest a different mechanism for the film's cohesion than ligand interactions. As demonstrated by x-ray measurements, our self-assembled film on water has an in-plane crystalline domain size of only ~40 nm [3]. This is considerably smaller than domain sizes in the freestanding film—self-assembled by drying a droplet of oil-nanoparticle suspension—which are in the tens of microns [18]. Moreover, our film, while optically homogeneous, is peppered with micron-sized vacancies [Fig. 3(a)] caused by the imperfect annealing of adjacent clusters during compression [Fig. 1(a)]. Thus, our film is expected to be weaker than films with larger crystalline domain size and fewer defects. Note that defects alone should not alter the relationship $B \propto Et^3$ [19].

We now examine the wrinkles in the trilayer film. The relations in Eqs. (1) and (2) are derived in the quasistatic, inextensible limit; i.e., dynamics or surface tension does not play a role. To test these assumptions for our system, we measured λ of the trilayers on subphases of pure glycerol and of a water-ethanol solution [Figs. 3(a), 3(b), and 4]. Changing the subphase to glycerol of viscosity $\eta_g = 1500$ cP (for water, $\eta_w = 1$ cP) does not prevent the film from wrinkling and V folding. The wavelength of the nanoparticle film on pure glycerol is 2.5 ± 0.4 μm, as measured over 300 wrinkles. Likewise, wrinkles and V folds occur on the surface of a water-ethanol solution (air-liquid surface tension $\gamma = 40$ mN/m; for pure water $\gamma = 72$ mN/m) [12]. The film wrinkles with a wavelength of 2.7 ± 0.5 μm (measured on over 300 wrinkles).

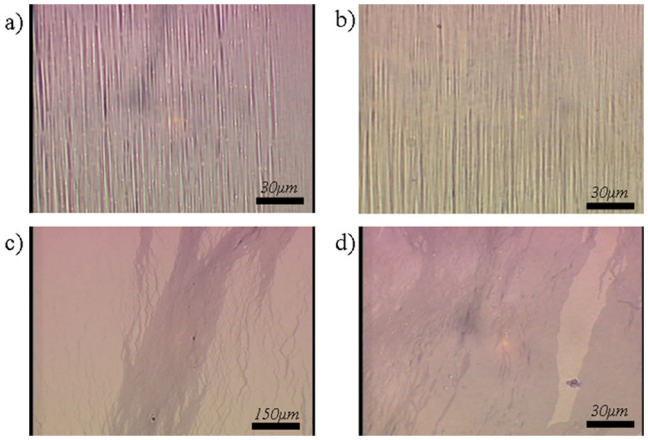

FIG. 3 (color online). Wrinkles of the nanoparticle film are visible on a high-viscosity pure glycerol subphase (a) and a low-surface-tension water-ethanol subphase (b). Folds are also visible for films on glycerol or water-ethanol subphases. (c, d) Adding free ligands to the gold suspension completely suppresses wrinkles and V folds. Collapse structures in (c, d) are an order of magnitude larger than wrinkles or folds and no longer localized or unidirectional.

Since glycerol is slightly denser than water ($\rho_g/\rho_w = 1.26$), λ is expected to be 2.5 μm according to Eq. (2), if B is assumed to be the same as that of the film on water. This value agrees with the measured λ, suggesting that the continuum treatment in Eq. (1) is valid. Moreover, there is no observed difference in the wrinkle wavelength between the films on a pure water subphase and those on a water-ethanol subphase, in spite of a factor of 2 change in the interfacial energy. This is in agreement with the theo-

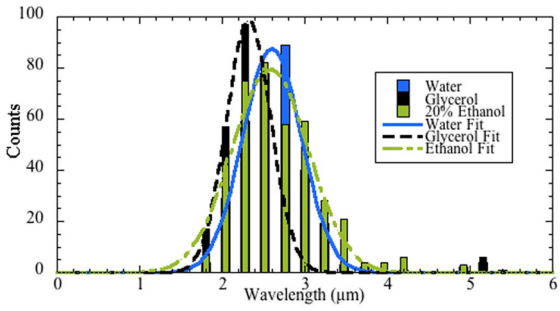

FIG. 4 (color online). Normalized histogram of wrinkle wavelengths of the gold nanoparticle film. The blue bars represent wrinkle wavelengths of the film on a pure water subphase (mean ± standard deviation = 2.7 ± 0.5 μm); the olive and black bars represent wrinkle wavelengths of the film on an 80/20 water-ethanol subphase and a pure glycerol subphase (2.7 ± 0.5 μm and 2.5 ± 0.4 μm), respectively. The lines represent fits of the data to Gaussians.

retical model [see Eq. (1)] where the wavelength does not depend on the surface tension. Our data affirm the continuum treatment of Eqs. (1) and (2) and evidence that wrinkle wavelength in our film is insensitive to the viscosity and the surface tension of the subphase, and is solely determined by the subphase's static resistance to deformation.

Inversion of Eq. (2) for the nanoparticle films yields a value of $B \approx 0.1$ kT, using the measured wavelength and the known substrate density [20]. Physically, the bending rigidity of the trilayer is determined by the bending rigidity of the individual layers, the resistance to stretching or compression of the outer layers, and the amount of coupling between layers. If there were no coupling between layers, then $B = NB_0$, where B_0 is the bending rigidity of each of the N individual layers. For the nanoparticle trilayer, this still leads to an anomalously small B. If the layers were perfectly coupled, then B would be that of a continuum plate, or $B \propto Et^3$. Using this relation and $E \approx 40$ MPa as estimated above, however, gives a value of $B \approx 3 \times 10^3$ kT, which is 4 orders of magnitude larger than the value derived from Eq. (2). Our findings therefore point to poor out-of-plane coupling between the layers. This suggests that, while the continuum approach motivating Eq. (2) is valid, the continuum expression for B is not for our film.

To test the idea that coupling between the layers affects the geometry of the trilayers, we have altered the interlayer coupling by adding excess ligands to the nanoparticle suspension as a plasticizer [12]. X-ray studies have previously shown that dissolving extra dodecanethiol in the film increases the nanoparticle separation, with the excess ligands encapsulating the particles [3]. This arrangement appears to reduce the film's resistance to shear and weakens the coupling between layers. As a result, the film's cohesive energy decreases, and it becomes too fluidlike to support wrinkling or V folding. Instead, the film responds to stress by forming large multilayer patches. These patches respond to further strain by shearing into collapse structures that are neither localized nor unidirectional; continued compression merely increases the size of these patches [Figs. 3(c) and 3(d)]. Similar in-plane relaxation is displayed by certain lipid monolayers with low resistance to shear [13]. This supports the idea that poor out-of-plane coupling between layers causes the nanoparticle trilayers to bend easily. Our results indicate that interlayer coupling provides another knob for tuning the materials properties of these thin nanoparticle films, in addition to altering the ligand length [2].

The highly localized, symmetry-broken V folded state was identified and reported earlier [5,9]. This wrinkle-to-folding transition has been described using a nonlinear geometric term in the elastic energy of the system, resulting in a scaling relation between the fold subducted length l and the wrinkle wavelength: $l \sim \lambda$. While this scaling has been verified for macroscopic wrinkled films on a subphase, its validity for systems at the nanometer scale has yet to be tested directly. For the gold nanoparticle film on water, the measured l (5–9 μm) is about 2 or 3 times the measured λ (2.7 μm), in qualitative agreement with the scaling argument in Ref. [5]. Similar folded states have been identified at other ''soft'' interfaces, such as on soft, highly compressed gels [21] and polymer films bound to a foam [21], however without a prior wrinkled stage.

We thank C. Penicka for experimental help and S. Rice for the lending of his equipment and fruitful discussions. This work was supported by the University of Chicago MRSEC of the NSF (DMR-0820054), the March of Dimes (No. 6-FY07-357), the U.S.-Israel Binational Science Foundation (No. 2006076), the NSF Inter-American Materials Collaboration: Chicago-Chile, the University of Chicago MTSP (NIGMS/MSNRSA 5T32GM07281), and ChemMatCARS (NSF/DOE, Grant No. CHE-0822838).

*To whom all correspondence should be addressed: lin@cars.uchicago.edu

[1] J. R. Heath, C. M. Knobler, and D. V. Leff, J. Phys. Chem. B **101**, 189 (1997); M. K. Bera *et al.*, Europhys. Lett. **78**, 56 003 (2007).
[2] U. Landman and W. D. Luedtke, Faraday Discuss. **125**, 1 (2004); G. U. Kulkarni, P. J. Thomas, and C. N. R. Rao, Pure Appl. Chem. **74**, 1581 (2002).
[3] D. G. Schultz *et al.*, J. Phys. Chem. B **110**, 24 522 (2006).
[4] S. T. Milner, J. F. Joanny, and P. Pincus, Europhys. Lett. **9**, 495 (1989).
[5] L. Pocivavsek *et al.*, Science **320**, 912 (2008).
[6] H. Diamant *et al.*, Phys. Rev. E **63**, 061602 (2001); P. Cicuta and D. Vella, Phys. Rev. Lett. **102**, 138302 (2009).
[7] T. A. Witten, Rev. Mod. Phys. **79**, 643 (2007).
[8] E. Cerda and L. Mahadevan, Phys. Rev. Lett. **90**, 074302 (2003).
[9] L. Pocivavsek *et al.*, Soft Matter **5**, 1963 (2009).
[10] Q. Zhang and T. A. Witten, Phys. Rev. E **76**, 041608 (2007).
[11] R. Huang and Z. Suo, J. Appl. Phys. **91**, 1135 (2002).
[12] See supplementary material at http://link.aps.org/supplemental/10.1103/PhysRevLett.105.058301 for experimental details.
[13] L. Pocivavsek *et al.*, Soft Matter **4**, 2019 (2008).
[14] K. Y. C. Lee *et al.*, Langmuir **14**, 2567 (1998).
[15] L. Landau and L. M. Lifshitz, *Theory of Elasticity* (Pergamon, New York, 1986), 3rd ed..
[16] S. Mora *et al.*, Europhys. Lett. **66**, 694 (2004); R. Goetz, G. Gompper, and R. Lipowsky, Phys. Rev. Lett. **82**, 221 (1999).
[17] K. Mueggenburg *et al.*, Nature Mater. **6**, 656 (2007).
[18] S. Narayanan, J. Wang, and X.-M. Lin, Phys. Rev. Lett. **93**, 135503 (2004).
[19] D. Vella, P. Aussillous, and L. Mahadevan, Europhys. Lett. **68**, 212 (2004).
[20] The value for E in Ref. [5] was based on preliminary measurements and assumed perfect coupling between layers.
[21] V. Trujillo, J. Kim, and R. C. Hayward, Soft Matter **4**, 564 (2008); P. M. Reis *et al.*, Phys. Rev. Lett. **103**, 045501 (2009).